Diffraction refinement of localized antibonding at the Si(111) 7×7 surface

J. Ciston,[1] A. Subramanian,[1] I. K. Robinson,[2] and L. D. Marks[1]

[1]*Department of Materials Science and Engineering, Northwestern University, Evanston, Illinois 60208, USA*
[2]*Department of Physics and Astronomy and London Centre for Nanotechnology, University College London, London WC1H 0AH, United Kingdom*

We report an experimental refinement of the local charge density at the Si(111) 7×7 surface using a combination of x-ray and high-energy electron diffraction. This method can be generally applied to the charge-density refinement at surfaces of other materials. By perturbing about a bond-centered pseudoatom model, we find experimentally that the adatom electrons occupy antibonding-like backbond states with the atoms below. We are also able to refine a charge transfer of 0.26 ± 0.04 e^- from each adatom to the underlying layers, in agreement with full-potential density-functional theory calculations.

Two of the most powerful techniques for determining structures are x-ray diffraction and transmission electron microscopy or diffraction. It is very well established that in the bulk these techniques can be used not just to determine atomic positions, but going beyond this to measure local charge-density variations.[1,2] At any surface one of the most important scientific issues is the local redistribution of electron density, not simply the atomic positions, since the electron density governs most of the behavior and plays a central role in many properties of scientific and technological importance.

Perhaps the most interesting and challenging monospecies surface structure is the Si(111) 7×7 reconstruction first observed by Schiller and Farnsworth[3] and finally solved decades later by Takayanagi *et al.*[4,5] who proposed the well-known dimer, adatom, stacking fault (DAS) structure. The large size of this structure has provided a challenge to density-functional theory (DFT) calculations with the first *ab initio* relaxations and surface energy computations utilizing local-density approximation (LDA) (Ref. 6) pseudopotential methods not appearing until 1992.[7,8] The first generalized gradient approximation (GGA) (Ref. 9) pseudopotential DFT calculations of the DAS structure did not appear until 2005 and is qualitatively consistent with the earlier LDA results. This structure has also played an important role in the development of scanning probe techniques, both in their infancy[10] and in pushing the limits past atomic resolution in AFM measurements of bond energies[11] to subatomic resolution in scanning tunneling microscopy (STM) studies where the out-of-plane adatom orbitals were resolved distinctly.[12,13]

In this Brief Report, we present a surface diffraction refinement of site-specific charge transfer at the Si(111) 7×7 surface, which pushes the limit of the amount of information a combination of x-ray and transmission high-energy electron-diffraction data can provide. By perturbing about a bond-centered pseudoatom model, we find experimentally that the adatoms are in an antibonding state with the atoms directly below which may finally explain the anomalous height of the adatom above the surface.[14] We are also able to experimentally refine a charge transfer of 0.26 ± 0.04 e^- from each adatom site to the underlying layers. These experimental results are compared with all-electron full-potential DFT structural refinements.

The x-ray measurements were conducted at X16A beamline at the National Synchrotron Light Source at Brookhaven National Laboratory. We used a $6 \times 30 \times 0.2$ mm³ Si(111) wafer slice, which was first etched with HF to grow a controlled oxide layer. Then it was flashed by passage of current to 1200 C for 5 s, cooled very quickly to about 900 C then slowly to 750 C, spanning the phase-transition region. The pressure in the chamber during the measurements lasting 84 h was around 5×10^{-10} torr. 1054 symmetry-reduced structure factors were measured by numerical integration of rocking scans about each point in reciprocal space, wide enough to allow a full background subtraction, then corrected for Lorentz factor, polarization, and active area.[15]

For the electron diffraction measurements, undoped Si(111) single crystal samples were cut into 3 mm disks and mechanically dimpled then thinned to electron transparency by a HF and HNO_3 chemical etch. These samples were then transferred into a UHV chamber with a base pressure of 8×10^{-11} torr and annealed by electron bombardment for 20 min at 720 C to produce the 7×7 reconstruction. Samples were transferred *in situ* to a Hitachi UHV-H9000 transmission electron microscope for off-zone-axis parallel nanobeam diffraction experiments. A total of 3540 in-plane measurements were reduced to 77 $p3m1$ symmetry unique reflections ($p6mm$ Patterson symmetry) using a Tukey-biweight method to a resolution of 0.65 Å^{-1}.

Two independent refinements were carried out utilizing different sets of silicon scattering factors. For the first refinement, isolated atomic form factors (IAM) were treated according to the expansion of Su and Coppens;[16] these were transformed to electron-scattering factors utilizing the Mott-Bethe formula. The global bonding charge density was addressed in a second refinement using a bond-centered pseudoatom (BCPA) formalism which treats the $1s$, $2s$, and $2p$ core electrons identically to the IAM model, applies a fixed modified Slater orbital expansion for the $3s$ and $3p$ valence states, and utilizes distorted bulk parameterization of the Si-Si bond density with Gaussian charge clouds as described in Refs. 17 and 18. By utilizing a BCPA model to parametrize the bond charges as a function of only the bond length, one may refine the global surface charge density without the addition of adjustable parameters to the refinement.

Diffraction refinements were performed utilizing a robust degree of freedom reduced χ figure of merit scaled for intensity conservation. A modified robust Hamilton R-test was used to assess the statistical significance of adding adjustable parameters to the fit. For the combined x-ray and electron case, there were 1131 independent data points and 129 adjustable parameters: 114 for nonsymmetry constrained positions of 49 atoms, 4 temperature factors (only the adatoms treated with separate in- and out-of-plane terms), and 11 scaling terms yielding 1002 degrees of freedom. The refined model consisted of 61 atoms representing the addition of one 12-atom layer constrained to bulk positions at the bottom surface. No preferential weighting was given to the electron data set and all data were weighted according to the inverse of their errors. Although electron-diffraction data are in principle more sensitive to bonding because small perturbations to bonding electrons induce large changes in the screening of the core potential, the electron data set was not large enough to be used alone due to the large number of parameters required to fully describe this structure. It is important to note that the diffraction refinement did not utilize any information from the DFT structural relaxation presented later.

To confirm the sensitivity to the diffraction data to bonding effects, the BCPA model was applied globally to the system as a whole which yielded a reduction in the refined χ from an IAM value of 2.689 to 2.599 for the bonded case. This reduction in χ is statistically significant to over 99.999% due to the large number of degrees of freedom. When only the x-ray data set was used, the improvement in χ due to the BCPA bonding approximation was similar. The RMS deviation of the IAM-refined atomic positions from the BCPA refined positions was 0.035 Å. As expected, the inclusion of subtle bonding effects has relatively little impact on the atomic positions as x-ray scattering is dominated by the core electrons. CIF files of the Si(111)-7×7 structures refined to the diffraction data set and DFT relaxation are available online in the EPAPS repository.[19]

Once a global correction to the valence charge density has been applied, it is possible to probe more subtle site-specific perturbations about the BCPA charge density. The first feature to be examined was the nature of the bond between the adatoms and the atomic sites directly below. To probe this, we performed refinements for four distinct cases:

(a) adatoms are threefold coordinated and not bonded to the third layer;

(b) adatoms are fourfold coordinated and bonded via a BCPA feature to the third layer;

(c) adatoms are fourfold coordinated and exhibiting an antibonding state with the third layer atoms (via a BCPA feature with the backbond length, but opposite sign)—essentially adding a "dangling bond" above the adatoms;

(d) all the adatoms, rest atoms, and the hole atom have a dangling bond, where the effective distance for the rest atoms and hole atom was taken as the mean of the adatoms.

In each of these cases, all of the other Si-Si pairs were treated under the BCPA formalism. We found from the diffraction refinement that case c, an antibonded adatom, was the most favorable to a 96% confidence level. This configuration of the adatom orbitals is consistent with prior AFM (Ref. 11) and STM (Refs. 12 and 13) studies of this surface.

While based solely upon the refinement we cannot fully justify adding a dangling bond to the rest and hole atoms (c and d were indistinguishable), physically it is more reasonable to assume that they are chemically similar. The adatom dangling bonds of case c are interpreted as an antibonding state due to the close proximity (2.85 Å) to the atoms directly below (see Fig. 1). Conversely, the rest atoms and corner hole atoms are 4 Å distant from the atoms below, so this is interpreted as merely a dangling unpaired electron rather than an antibond. Case b was the worst performing in the diffraction refinement due to the unstable fivefold coordination of the third layer backbond. Refinements of the various backbonding states became degenerate when the electron diffraction portion of the data was removed from the refinement, which was not surprising; adding a dangling bond delocalizes the electron density which will increase the electrostatic potential, even in projection, to which the TED data are very sensitive.

We next turned to the refinement of a feature with a predominantly in-plane component: charge transfer from the adatom sites to/from the underlying tripod atoms (see Fig. 1). When the charge transfer at all four adatom sites was constrained to be identical, the value refined to be 0.26 ± 0.04 e^- per adatom. Application of the Hamilton R-test to determine if the addition of this adjustable parameter was allowed yielded a confidence value of 99%. Although the adatoms represent only 12 of the 249 atoms in the refined structure, the data are extremely sensitive to charge defects fractions of an electron in magnitude. An attempt was made to refine the adatom charge transfer against the x-ray data alone, but this refinement proved unstable.

Another unusual feature of the DAS structure are the buried dimer atoms which have previously been shown to exhibit bond lengths $6 \pm 2\%$ longer than bulk values,[20] indicating a slightly weaker bond compared to the bulk. We have refined the value of the dimer bond density against the diffraction data to be 0.37 ± 0.04 e^- (92% of the bulk value) by allowing the charge clouds within the BCPA model to vary in magnitude with all dimers treated identically. The refined magnitude of the dimer bond was invariant to the application of charge transfer to the adatom bond indicating that these two site-specific parameters are independent variables. Although the dimer bond refinement was stable, the addition of the adjustable parameter for dimer bond strength failed the Hamilton test with a confidence value of $<40\%$ meaning the dimer bond refinement is suggestive rather than definitive. Refinement of the dimer strength against only the x-ray data set yielded a significant reduction in χ, but the value of the dimer bond diverged and produced values of $5-7$ e^- which is unphysical.

We also performed a DFT structural relaxation using the all-electron WIEN2K code[21] with the exchange correlation contribution approximated using the PBE96 GGA functional[9] as well as the more accurate functional due to Tao, Perdew, Staroverov, and Scuseria[22] (TPSS) used only for a correction to the total energy after a GGA relaxation. Prior experience has shown that the absolute energy error in PBE surface calculations can be approximated by the difference in the total energy between the PBE and TPSS functionals.[23] DFT surface energies may be found in Table I.
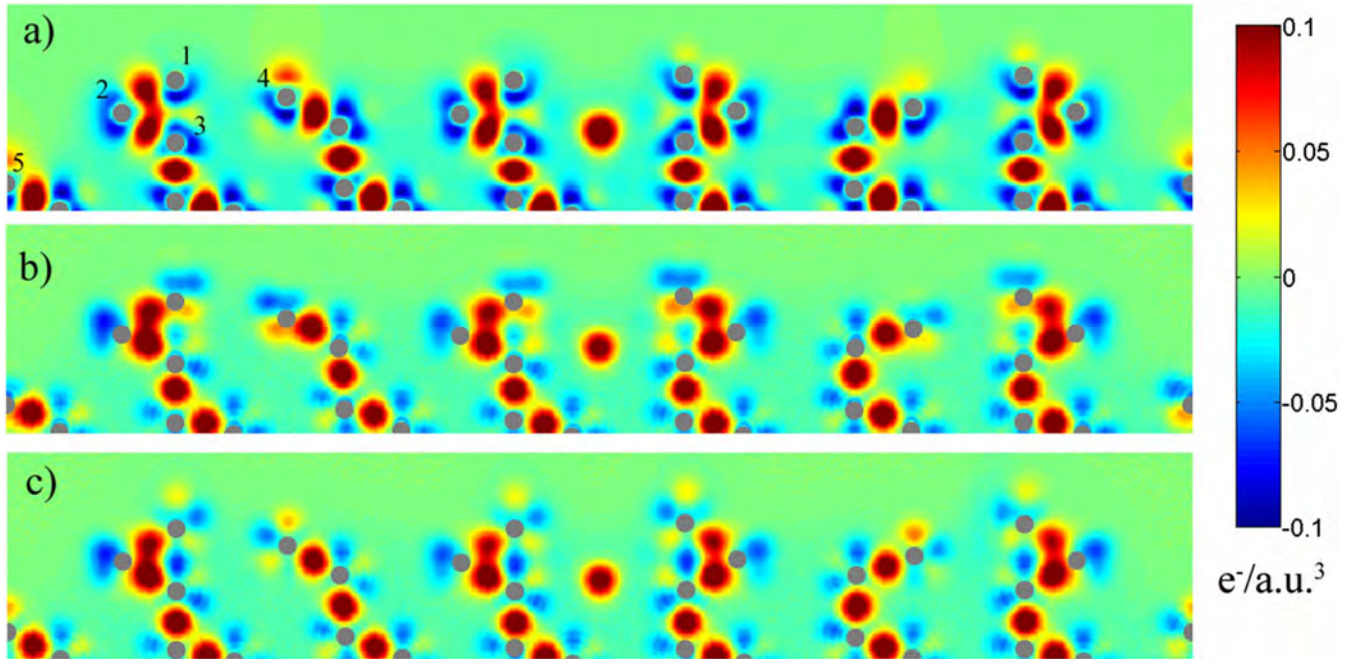
FIG. 1. (Color online) (110) slice through 7×7 unit cell of (a) the DFT difference density, (b) the diffraction-refined difference density using just the conventional BCPA, and (c) a map of the charge-density features fitted in the diffraction refinement including both the dangling bond features as well as the charge transfer. Silicon atom positions are shown in gray. Color scale is electrons per cubic atomic unit. Atoms labeled as follows: (1) adatom, (2) tripod atom, (3) backbond atom, (4) rest atom, and (5) corner hole atom.

The unit cell used was 26.882 Å $\times$ 26.882 Å $\times$ 28.220 Å (a 1.25% volume expansion relative to the experimental unit cell as determined by a total energy volume optimization). The surface slab was centrosymmetric and comprised of 12 layers, 61 independent atoms with P-$3m1$ symmetry (498 total atoms), and 10 Å of vacuum between surfaces. All atoms were free to move during the relaxation including the central unreconstructed layers. Technical parameters for the calculation were Si muffin-tin radii of 2.12, an RKMAX of 6.75, and a single k point at the special point (5/18,1/9,0). The structure was relaxed until all forces acting on the atoms were under 0.2 eV/Å. All calculations were performed spin unpolarized as the spin-zero closed shell state has previously been calculated to be the ground state for the 7×7-DAS structure.[24]

The RMS in-plane deviation of experimentally refined atomic positions with respect to the relaxed DFT values was 0.08 Å. However, the out-of-plane performance was not as good with an RMS deviation from DFT values of 0.27 Å mostly due to excess outward relaxation of the surface layers in the diffraction refinement. This reflected the fact that the in-plane electron-diffraction data had much smaller errors

than the comparable x-ray data sets and also that the in-plane x-ray data were of higher quality than the out-of-plane rod scans. The out-of-plane uncertainty was also exhibited in the refined temperature factors of the adatom layer with B values of 15 Å^2 in the out-of-plane direction and 0.92 Å^2 in plane. A portion of this quite large value was due to an accumulation of collective out-of-plane vibrations from the underlying layers.

To assess the magnitude of charge transfer to/from the adatom sites, the total DFT electron density was integrated over each atomic basin utilizing the Bader atoms in molecules[25] (AIM) approach coded into the WIEN2k package. The average charge transfer determined from DFT was 0.16 ± 0.03 e^- per adatom, similar to the experimentally refined value of 0.26 ± 0.04 e^-. Note that the diffraction refinement addressed the charge at each atomic site by directly transferring density from the spherical component of the $3sp$ shell of one atom to that of another, whereas AIM analysis is a method of partitioning the global charge density of the structure to individual atoms. While the AIM method can be somewhat misleading in assigning electrons from the total charge density as "belonging" to particular atoms, it allows qualitative verification that the magnitude and direction of the diffraction-refined charge transfer is reasonable. AIM analysis may also be used to determine the "strength" of a bond by looking at the charge density at the bond critical points. We found the DFT density of the dimer bond to be 93% of the bulk value. This is in remarkable agreement to the value of 92% refined against the diffraction data.

A (110) slice through the charge density of the 7×7 surface cell allows for visualization of all of the symmetry-inequivalent adatoms, rest atoms, and corner holes. A plot of

TABLE I. DFT surface energies per 1×1 unit cell.

Method	eV/1×1
PBE full potential	0.954
TPSS full potential	0.949
PBE pseudopotential[24]	1.044
LDA pseudopotential[8]	1.153

the difference between the full DFT charge density and the charge density of superpositioned isolated atoms is shown in Fig. 1(a) and compared with in Fig. 1(b), a difference map just using the BCPA model with no dangling bonds and in Fig. 1(c) with dangling bonds on the adatoms, rest atoms, hole atom and the charge transfer described above. We did not refine against the DFT data, but argue the fact that Figs. 1(a) and 1(c) are qualitatively much more similar than Figs. 1(a) and 1(b) supports a contention that we are refining here physically significant features in the density, not overfitting noisy data. A closer inspection of the DFT difference density at the adatoms revealed that the adatom charge density is qualitatively similar to a Si-Si antibond as indicated by the wedge of off-axis excess charge. This confirmed the aforementioned finding of the diffraction refinement which favored an antibonded adatom backbond.

In this study we have been able to refine the first three-dimensional site-specific surface charge density from diffraction data. Although the x-ray diffraction data were shown to be globally sensitive to bulk valence charge-density effects, these experiments alone appear insufficiently sensitive to refine site-specific perturbations to the bonding at the surface. Electron diffraction was shown to be more sensitive to local bonding effects, but does not generally provide a sufficiently large data set for the refinement of a structure of this size. The application of these two powerful structural characterization techniques in combination acts synergistically to enable the simultaneous refinement of precise atomic positions and minute changes in occupation of highly diffuse valence bonding orbitals. The methodology of combining these two experimental techniques, along with the use of a highly accurate starting model for the valence charge density about which local perturbations can be addressed, is generally applicable to other materials and may open new avenues to the understanding of bonding at unusually coordinated surfaces.

[1] T. S. Koritsanszky and P. Coppens, Chem. Rev. **101**, 1583 (2001).

[2] J. M. Zuo, M. Kim, M. O. O'Keeffe, and J. C. H. Spence, Nature (London) **401**, 49 (1999).

[3] R. E. Schlier and H. E. Farnsworth, J. Chem. Phys. **30**, 917 (1959).

[4] K. Takayanagi, Y. Tanishiro, M. Takahashi, and S. Takahashi, J. Vac. Sci. Technol. A **3**, 1502 (1985).

[5] K. Takayanagi, Y. Tanishiro, S. Takahashi, and M. Takahashi, Surf. Sci. **164**, 367 (1985).

[6] J. P. Perdew and Y. Wang, Phys. Rev. B **45**, 13244 (1992).

[7] K. D. Brommer, M. Needels, B. E. Larson, and J. D. Joannopoulos, Phys. Rev. Lett. **68**, 1355 (1992).

[8] I. Stich, M. C. Payne, R. D. King-Smith, J. S. Lin, and L. J. Clarke, Phys. Rev. Lett. **68**, 1351 (1992).

[9] J. P. Perdew, K. Burke, and M. Ernzerhof, Phys. Rev. Lett. **77**, 3865 (1996).

[10] G. Binnig, H. Rohrer, C. Gerber, and E. Weibel, Phys. Rev. Lett. **50**, 120 (1983).

[11] M. A. Lantz, H. J. Hug, R. Hoffmann, P. J. A. van Schendel, P. Kappenberger, S. Martin, A. Baratoff, and H. J. Guntherodt, Science **291**, 2580 (2001).

[12] F. J. Giessibl, S. Hembacher, H. Bielefeldt, and J. Mannhart, Science **289**, 422 (2000).

[13] A. N. Chaika and A. N. Myagkov, Chem. Phys. Lett. **453**, 217 (2008).

[14] T. Hanada, S. Ino, and H. Daimon, Surf. Sci. **313**, 143 (1994).

[15] I. K. Robinson, in *Handbook on Synchrotron Radiation*, edited by D. E. Moncton and G. S. Brown (Elsevier/North-Holland, New York/Amsterdam, 1990), Vol. III.

[16] Z. W. Su and P. Coppens, Acta Crystallogr. A **54**, 646 (1998).

[17] J. Ciston, L. D. Marks, R. Feidenhans'l, O. Bunk, G. Falkenberg, and E. M. Lauridsen, Phys. Rev. B **74**, 085401 (2006).

[18] L. D. Marks, J. Ciston, B. Deng, and A. Subramanian, Acta Crystallogr. A **62**, 309 (2006).

[19] See EPAPS Document No. E-PRBMDO-79-134915 for cif files. For more information on EPAPS, see http://www.aip.org/pubservs/epaps.html.

[20] I. K. Robinson, W. K. Waskiewicz, P. H. Fuoss, and L. J. Norton, Phys. Rev. B **37**, 4325 (1988).

[21] P. Blaha, K. Schwartz, G. K. H. Madsen, D. Kvasnicka, and J. Luitz, *An Augmented Plane* Wave+Local *Orbitals Program for Calculating Crystal Properties* (Karlheinz Schwarz, Techn Universität Wien, Austria, 2001).

[22] J. M. Tao, J. P. Perdew, V. N. Staroverov, and G. E. Scuseria, Phys. Rev. Lett. **91**, 146401 (2003).

[23] J. Ciston, A. Subramanian, and L. D. Marks, Phys. Rev. B **79**, 085421 (2009).

[24] S. D. Solares, S. Dasgupta, P. A. Schultz, Y. H. Kim, C. B. Musgrave, and W. A. Goddard, Langmuir **21**, 12404 (2005).

[25] R. F. W. Bader, *Atoms in Molecules-A Quantum Theory* (Oxford University Press, Oxford, 1990).